

Fermion and spin counting in strongly correlated systems

Sibylle Braungardt,¹ Aditi Sen(De),¹ Ujjwal Sen,¹ Roy J. Glauber,² and Maciej Lewenstein^{1,3}
¹*ICFO—Institut de Ciències Fotòniques, Mediterranean Technology Park, 08860 Castelldefels (Barcelona), Spain*
²*Lyman Laboratory, Physics Department, Harvard University, Cambridge, Massachusetts 02138, USA*
³*ICREA—Institució Catalana de Recerca i Estudis Avançats, 08010 Barcelona, Spain*

(Received 11 June 2008; revised manuscript received 12 August 2008; published 18 December 2008)

We apply the atom counting theory to strongly correlated Fermi systems and spin models, which can be realized with ultracold atoms. The counting distributions are typically sub-Poissonian and remain smooth at quantum phase transitions, but their moments exhibit critical behavior, and characterize quantum statistical properties of the system. Moreover, more detailed characterizations are obtained with experimentally feasible spatially resolved counting distributions.

DOI: 10.1103/PhysRevA.78.063613

PACS number(s): 67.85.-d, 05.30.Fk, 75.10.Pq

I. INTRODUCTION

A. Particle and spin counting

Particle-wave duality is one of the most spectacular and at the same time intriguing phenomena of quantum mechanics. Nevertheless, careful counting of particles, such as photons, in a given quantum mechanical state allows one to fully reconstruct the wave nature and coherence properties of the state. The formulation of photon-counting theory in the frame of quantum electrodynamics was done in Ref. [1]. Recent progress in physics of ultracold atoms made it possible to develop and apply techniques of single-atom counting to various systems. Since the pioneering experiments of Shimizu [2], spectacular measurements of the Hanbury-Brown–Twiss effect for bosons [3] and fermions [4] have been performed with ultracold metastable helium atoms. Esslinger and co-workers group employed cavity quantum electrodynamics techniques to measure the pair correlation function in an atom laser beam outgoing from a trapped Bose-Einstein condensate [5]. These new detection methods allow one in principle to measure full atom-counting distributions with spatial resolution (by counting only atoms in a certain spatial region), and provide novel efficient ways of detection of strongly correlated systems [6]. Shot noise and counting statistics for expanding gases has been recently considered in Ref. [7].

Equally spectacular progress has been achieved in spin counting, or in other words, measurements of total atomic spin for atoms with spin or pseudospin degrees of freedom. The idea of quantum nondemolition polarization spectroscopy (QNDPS) has been demonstrated in Ref. [8]. It employs the quantum Faraday effect: a polarized light beam passed through the atomic sample undergoes polarization rotation. Atomic fluctuations leave an imprint on the quantum fluctuations of the light, and vice versa. This idea was recently extended to ultracold spinor gases [9], where it can be used to detect, manipulate, and even engineer various states of such systems. The Hamiltonian describing the QNDPS is very simple:

$$H = \chi S_z J_z. \quad (1)$$

Here χ is the coupling constant proportional to the optical density of the sample, S_z is the z component of the total

atomic spin, and J_z is the z component of the so-called Stokes vector [10], given by the difference between the number of right and left polarized photons in the light beam. What is measured are the fluctuations of the other two Stokes parameters, J_x and J_y , which contain directly a part proportional to the fluctuations of S_z .

Amazingly, this method also allows for spatial resolution (when standing laser beams are employed) [11]. In this case the Hamiltonian becomes

$$H = \chi S_z^{\text{eff}} J_z, \quad (2)$$

where $S_z^{\text{eff}} = \int d\mathbf{x} s_z(\mathbf{x}) \cos^2(\mathbf{k}_L \mathbf{x})$ is the “effective” component of the total atomic spin, given by the integral of the spin density $s_z(x)$ with the intensity profile of the standing wave, with k_L being the wave vector. In this case, the measurement of J_x and J_y allows measurement of the fluctuations of S_z^{eff} , i.e., of a combination of the zero and $\pm 2k_L$ Fourier components of the spin density.

B. Main results

In this paper, we show how the atom-counting techniques can be used to detect properties of strongly correlated systems. We concentrate, in particular, on the case of fermion and/or spin counting in one-dimensional (1D) optical lattices, which are equivalent, via Jordan-Wigner transformation [12], to 1D spin chains. The problem of spin counting for a local block of spins in the 1D Ising model in a transverse field has been considered by Cherng and Demler [13]. Our paper is in a sense complementary to Ref. [13]. First, we consider the counting statistics not only on the Ising model, but on the whole family of asymmetric XY models, characterized by the asymmetry (or anisotropy) parameter γ , in the transverse field h . Second, employing ideas of Ref. [11], we calculate not only the counting distribution for the total fermion number (total Z-spin component), but also for the “effective” number, corresponding to certain spatial Fourier components of the fermion (spin) density [see Eq. (2)]. While for the considered family of models counting distributions are always smooth, their cumulants exhibit critical behavior at $h = h_c$, evident even for small detection efficiencies. For the antiferromagnetic spin models, the distributions are typically sub-Poissonian, but their sub-Poissonian character

changes, as we sweep h from 0 to ∞ . For small γ , the $h=0$ distribution is narrower than the distribution of $h=\infty$, while for large γ , the $h=0$ distribution is wider than that of $h=\infty$. This change of character can be used to define a “transition anisotropy,” which leads to a distinction between the two classes present in the family of XY models. For ferromagnetic spin chains, we observe a transition from sub- to weakly super-Poissonian as we change h . The transition occurs at h_t , and $h_t \rightarrow h_c$, as $\gamma \rightarrow 0$. Also, quite generally, a transition from sub- to super-Poissonian occurs in the statistics with spatial resolution. Through the paper, we use a generalization of the photon-counting theory to fermions, derived by Cahill and Glauber within the formalism of Grassmann variables [14]. We obtain, for the cases we consider, analytic expressions for the counting distributions in terms of simple recursion relations.

Recently, counting statistics has also been considered for charged particles (electrons) in mesoscopic devices [15] (see also [16]). While the particles in Ref. [15] are practically noninteracting, in contrast we deal here with strongly interacting superfluid Fermi liquids and quantum phase transitions [12]. Counting statistics of many-body states of interacting fermionic systems have been considered in Refs. [17,18] in the context of Bose-Einstein condensate (BEC) to BCS transition. In Ref. [17], the counting statistics of the fermionic density was calculated in an interacting system of particles, within a mean field approach: a crossover from Poissonian to sub-Poissonian statistics was noticed. A similar question in another many-body system was addressed in Ref. [18], with the discussion being mainly about the density correlators. Note that the methods used in these references are different from than ours.

The paper is organized as follows. In Sec. II, we briefly describe the models of the 1D optical lattice that we consider, and the Jordan-Wigner transformation that can be used to diagonalize them. In the next section (Sec. III), we derive the counting statistics of fermions in the systems described by these models; in particular, we discuss them for the Ising model (Sec. III D), and more generally for the asymmetric XY model (Sec. III E). In Sec. III F, we consider the means and variances of the counting distributions: We derive recurrence relations that allow for easy calculation of these moments for an arbitrary number of particles and modes in the system. We discuss also the generalization of our method to the case of Fourier components of the total spin in Sec. III H. Finally, we summarize our results in Sec. IV.

II. FERMION GAS IN A 1D OPTICAL LATTICE

A. 1D Fermi gases

Let us consider a family of models describing a one-dimensional Fermi gas in an optical lattice, described by the Hamiltonian

$$H = -\frac{J}{2} \sum_{j=0}^{N-1} (c_j^\dagger c_{j+1} + \gamma c_j^\dagger c_{j+1}^\dagger + \text{H.c.} - 2g c_j^\dagger c_j), \quad (3)$$

where $J/2$ is the energy associated with fermion tunneling, $g=h/J$, and N is the number of sites. One way to realize such

a Hamiltonian with ultracold atoms is to use a Fermi-Bose mixture in the strong coupling limit. In this limit, the low-energy physics is well described by fermionic composite theory [19], in which fermions form composite objects with $0, 1, \dots$ bosons, or bosonic holes, respectively. The fermionic composites undergo tunneling and interact via nearest neighbor interactions, which may be repulsive or attractive, weak or strong, depending on the original parameters of the system, such as scattering lengths, etc. In the case of weak attractive interactions, the system undergoes, at zero temperature, a transition into a “ p -wave” superfluid, described well by the Bardeen-Cooper-Schrieffer (BCS) theory [20], corresponding exactly to the Hamiltonian (3).

B. 1D spin chains

We now use the Jordan-Wigner transformation [12] to obtain the Hamiltonian of a 1D asymmetric XY spin chain in the transverse magnetic field h , from the Hamiltonian in Eq. (3). First, we define operators

$$S_j^x = \frac{1}{2}(b_j^\dagger + b_j), \quad (4)$$

$$S_j^y = \frac{1}{2i}(b_j^\dagger - b_j), \quad (5)$$

$$S_j^z = \left(b_j^\dagger b_j - \frac{1}{2} \right), \quad (6)$$

which are related to the Fermi operators (c_i, c_i^\dagger) in the following way:

$$b_j = \exp\left(-\pi i \sum_{k=1}^{j-1} c_k^\dagger c_k\right) c_j, \quad (7)$$

$$b_j^\dagger = c_j^\dagger \exp\left(\pi i \sum_{k=1}^{j-1} c_k^\dagger c_k\right). \quad (8)$$

Applying the above transformations to the Hamiltonian, given in Eq. (3), we obtain

$$H_{xy} = J \sum_{j=0}^{N-1} \left((1 + \gamma) S_j^x S_{j+1}^x + (1 - \gamma) S_j^y S_{j+1}^y - \frac{h}{J} S_j^z \right), \quad (9)$$

where $S_j^\alpha = \frac{1}{2} \sigma_j^\alpha$ are the spin-1/2 operators at site j , proportional to Pauli matrices, and γ is the asymmetry (or anisotropy) parameter. The special cases $\gamma=0$ [i.e., the so-called symmetric (or isotropic) XY or XX limit] and $\gamma = \pm 1$ can be realized with single-species bosons in the hard core (i.e., strongly repulsive) bosons limit [12,21]. Another possibility is to use a chain of double-well sites filled with bosons interacting via weak dipolar forces [22]. In general, one should use a two-component Bose-Bose or Fermi-Fermi mixture in the strong coupling limit, and in the Mott insulator state with one atom per site. The two components provide then the two components of (pseudo)spin 1/2. Spin-spin interactions are induced by exchange mechanism via virtual tunnelings of

atoms [23–25]. The system is then described by an asymmetric (XXZ) Heisenberg model (cf. [21,26]) in the Z-oriented field. By appropriate tuning of the scattering lengths via Feshbach resonances, one can set the $S_{j+1}^z S_j^z$ coupling to zero, i.e., achieve the XX model in the transverse field. In order to achieve the asymmetry γ , one should additionally introduce tunneling assisted with a laser- or microwave-induced double spin flip. For this aim, one should make use of the resonance between the virtual on-site two atom “up-up” and “down-down” states, without disturbing “up-down” configurations.

C. Diagonalization

The Jordan-Wigner transformation, as is well known, works for open chains, and in particular for an infinite chain. We will nevertheless assume periodic boundary conditions to solve the fermion model (3) using Fourier and Bogoliubov transformations (see e.g. [27]). For large N , this procedure gives the right leading behavior. We define Fourier-transformed operators as

$$c_j^\dagger = \sum_{k=0}^{N-1} \exp(-ij\Phi_k) a_k^\dagger, \quad (10)$$

and

$$c_j = \sum_{k=0}^{N-1} \exp(ij\Phi_k) a_k, \quad (11)$$

where $\Phi_k = 2\pi k/N$. We perform then the Bogoliubov transforms

$$a_k = u_k d_k - iv_k d_{N-k}^\dagger, \quad a_k^\dagger = u_k d_k^\dagger + iv_k d_{N-k}, \quad (12)$$

where u_k and v_k are real numbers satisfying

$$u_k^2 + v_k^2 = 1,$$

$$u_{N-k} = u_k \quad \text{and} \quad v_{N-k} = -v_k, \quad (13)$$

so that we can write

$$u_k = \cos \frac{\theta}{2} \quad \text{and} \quad v_k = \sin \frac{\theta}{2}. \quad (14)$$

When

$$\tan \theta = \frac{\gamma \sin \Phi_k}{\cos \Phi_k - g}, \quad (15)$$

the Hamiltonian reduces to the noninteracting fermion Hamiltonian,

$$H = \frac{1}{2} \sum_{k=0}^{N-1} \epsilon_k d_k^\dagger d_k, \quad (16)$$

with

$$\epsilon_k = 2\sqrt{(\cos \Phi_k - g)^2 + \gamma^2 \sin^2 \Phi_k}. \quad (17)$$

The ground state is thus the vacuum of the d_k operators. For $\gamma > 0$ the spectrum is everywhere gapped (i.e., there is a nonzero difference between the ground state energy and the

energy of the first excited state), except at the critical point $g_c = 1$. For $\gamma = 0$, the d_k 's coincide with a_k 's or a_k^\dagger 's, and the ground state is a Fermi sea. For $-1 \leq g \leq 1$ the spectrum is then gapless and the system critical. Note that both the number of original fermions $\hat{N}_f = \sum_{i=0}^{N-1} c_i^\dagger c_i$, and the total Z component of the spin, $\hat{S}^z = \sum_{i=0}^{N-1} S_i^z = \hat{N}_f - 1/2$, are not conserved, except at $\gamma = 0$.

III. FERMION-COUNTING STATISTICS

A. Fermion-counting distributions

Let us now turn to counting procedures, and first of all ask what do we count? For the case of fermions, one should think about an approach analogous to the one used for the experiments on metastable helium [3,4], i.e., count atoms directly using the so-called multichannel plates. For spins, one could use QNDPS directly to measure the distribution of \hat{S}_z , or even its spatially resolved version \hat{S}_z^{eff} [11]. An alternative way would be to switch off the Hamiltonian (9) (by switching off the lasers), and induce spontaneous Raman transition from the state up to some side level. Counting of spontaneously emitted photons would correspond then to counting of up spins.

The next question is how to characterize the counting procedures. The standard approach for counting particles has been developed in Ref. [1] for photons absorbed in a photodetector. In this process, a photon is annihilated and a photoelectron emitted. This photoemission triggers a further ionization process, leading to a macroscopic current that is then measured. Mathematically, such absorption-based photodetectors are sensitive to the so-called normally ordered (i.e., creation operators to the left of the annihilation ones) and apex-ordered (growing times from left to right for creation, and decreasing for annihilation operators) correlation functions of the electric field that causes the photoemission (see, for instance, [28], and references therein). This special ordering is the consequence of the fact that ionization in the photodetector is caused by the positive frequency (i.e., annihilation) part of the electric field. The case of atoms is analogous: detectors based on absorption or, better to say, “destruction” of an atom (at the multichannel plate) are sensitive to the normally and apex-ordered correlation functions of atomic creation and annihilation fields. The situation is the same in the spin measurements using QNDPS, since the spin lowering and raising operators couple directly to the photon annihilation and creation operators, respectively, which then are measured by the standard photodetectors.

The quantity that is measured is the counting distribution, i.e., the probability $p(m, \tau)$ of counting m particles within a time interval τ . Since typically not all particles are counted, this quantity depends on the efficiency of the detectors η , or, better to say, on the product $\eta\tau$, which we will be denoting by κ . Note that κ is proportional to time only in the perturbative limit, when the detection does not affect the state. We assume that the counting measurement is performed either in the expanding cloud or in a nondemolition way, and the dynamics of the measurement will be fast in comparison to the dynamics of the system. Therefore, the measurement affects

the state only in the sense that the particles are annihilated during the detection, in which case, in a simplified model, κ is proportional to $1 - \exp(-\eta\tau)$ [28–30].

There exists a very elegant method of calculating $p(m)$ for photons using generating functions [1] (from now on we skip the τ dependence and include it in the parameter κ). The generating function approach was generalized by Cahill and Glauber for fermions [14]. The probability of detecting m particles in a given interval of time τ , and with efficiency per time η , can be expressed as the m th derivative with respect to a parameter λ of the generating function $\mathcal{Q}(\lambda)$ as

$$p(m) = \left. \frac{(-1)^m}{m!} \frac{d^m}{d\lambda^m} \mathcal{Q} \right|_{\lambda=1} \quad (18)$$

at $\lambda=1$, with $\mathcal{Q}(\lambda)$ being the expectation value of a normally ordered exponential $\mathcal{Q}(\lambda) = \text{Tr}(\rho : e^{-\lambda \mathcal{I}} :)$. For photons, the operator \mathcal{I} is given by the integral over the surface of the detector and over detection time interval of the factor $\eta \exp(-\eta\tau)$ times the intensity of light, i.e., a product of negative (creation) and positive (annihilation) frequency parts of the electric field operators (cf. [28]). If the latter product does not vary in time, the result is $\kappa = 1 - \exp(-\eta\tau)$ times the corresponding spatial integral of the light intensity. In the case of multichannel detection of atoms, the operator \mathcal{I} is given by $\eta \exp(-\eta\tau)$ times an integral over the detector surface and over detection interval of the product of the positive-frequency and negative-frequency parts of the quantum fields describing the particles to be counted. Again, if the latter product does not depend on time, the result is κ times a surface integral. For the case of QNDPS, the same expressions hold, although κ is now in a more complicated way related to χ of Eqs. (1) and (2) [31].

In the case of counting the total number of particles, we have

$$\mathcal{I} = \kappa \sum_{j=0}^{N-1} c_j^\dagger c_j = \kappa \sum_{j=0}^{N-1} \sigma_j^\dagger \sigma_j = \kappa \sum_{k=0}^{N-1} a_k^\dagger a_k.$$

For the spatially resolved QNDPS, $\mathcal{I} = \kappa \sum_{j=0}^{N-1} \sigma_j^\dagger \sigma_j \cos^2(\mathbf{k}_L \mathbf{r}_j)$, where \mathbf{k}_L is the wave vector of the standing wave used for detection, and \mathbf{r}_j is the position of the j th site.

For counting the total number of particles, $\mathcal{Q}(\lambda)$ can be written as

$$\mathcal{Q}(\lambda) = \text{Tr} \left[\rho : \exp \left(-\lambda \kappa \sum_{k=0}^{N-1} a_k^\dagger a_k \right) : \right]. \quad (19)$$

The operators $a_k^\dagger a_k$ commute for different k , and obey $a_k^\dagger a_k = (a_k^\dagger a_k)^2$ so that the expression for \mathcal{Q} can be rewritten as

$$\begin{aligned} \mathcal{Q}(\lambda) &= \text{Tr} \left(\rho : \prod_{k=0}^{N-1} (e^{-\lambda \kappa a_k^\dagger a_k}) : \right) \\ &= \text{Tr} \left(\rho : \prod_{k=0}^{N-1} (1 - \lambda \kappa a_k^\dagger a_k + \lambda^2 \kappa^2 a_k^\dagger a_k a_k^\dagger a_k + \dots) : \right) \\ &= \text{Tr} \left(\rho \prod_{k=0}^{N-1} (1 - \lambda \kappa a_k^\dagger a_k) \right) \end{aligned}$$

$$= \text{Tr} \left(\rho \prod_{k=1}^{N/2} (1 - \lambda \kappa a_k^\dagger a_k) (1 - \lambda \kappa a_{N-k}^\dagger a_{N-k}) \right),$$

as: $a_k^\dagger a_k a_k^\dagger a_k := a_k^\dagger a_k^\dagger a_k a_k = 0$, etc.

The terms $a_k^\dagger a_k$ and $a_{N-k}^\dagger a_{N-k}$ can then be expressed in terms of the d fermions:

$$a_k^\dagger a_k = (u_k d_k^\dagger + i v_k d_{N-k})(u_k d_k - i v_k d_{N-k}^\dagger),$$

$$a_{N-k}^\dagger a_{N-k} = (u_k d_{N-k}^\dagger - i v_k d_k)(u_k d_{N-k} + i v_k d_k^\dagger).$$

B. Generating function for the ground state

For fermions, the mean values of normally ordered products and the generating function $\mathcal{Q}(\lambda)$ can be calculated in a particularly convenient and elegant way using the Grassmann variable formalism, introduced in [14]. We consider the counting statistics of the c fermions in the ground state of the Hamiltonian, i.e., in the vacuum state of d fermions.

The trace in the generating function can now be easily calculated using Grassmann variable formalism [14]. The P representation for the density operator ρ is

$$\rho = \int d^2 \vec{\alpha} P(\vec{\alpha}) |\vec{\alpha}\rangle \langle \vec{\alpha}|, \quad (20)$$

where $|\vec{\alpha}\rangle$ are the fermionic coherent states, as defined in [14]. Using the P representation, the mean values of normally ordered products of d fermions can then be calculated as

$$\text{Tr}(\rho d_k^{\dagger n} d_l^m) = \int d^2 \vec{\alpha} P(\vec{\alpha}) \langle \vec{\alpha} | d_k^{\dagger n} d_l^m | \vec{\alpha} \rangle = \int d^2 \vec{\alpha} P(\vec{\alpha}) \alpha_k^{*n} \alpha_l^m, \quad (21)$$

where the α_i are Grassmann variables, and are defined by the eigenequation $d|\alpha_i\rangle = \alpha_i|\alpha_i\rangle$. For the vacuum state of the d fermions,

$$\rho = |0 \dots 0\rangle \langle 0 \dots 0|, \quad (22)$$

the P function is given by

$$P(\alpha) = \int d^2 \vec{\xi} \exp \left(\sum_i (\alpha_i \xi_i^* - \xi_i \alpha_i^*) \right) = \delta(\vec{\alpha}). \quad (23)$$

Evaluating Eq. (21) using Eq. (23), we get the relations

$$\text{Tr}(\rho d_k^{\dagger n} d_l^m) = \int d^2 \vec{\alpha} \prod_i (\alpha_i^*)^{n_i} \alpha_i^{m_i} \delta(\vec{\alpha}) = 0 \quad (24)$$

and

$$\text{Tr}(\rho) = \int d^2 \vec{\alpha} \delta(\vec{\alpha}) = 1. \quad (25)$$

The relevant remaining terms in the product $(1 - \lambda \kappa a_k^\dagger a_k)(1 - \lambda \kappa a_{N-k}^\dagger a_{N-k})$ in the generating function are thus

$$1 - \lambda \kappa v_k^2 d_{N-k} d_{N-k}^\dagger - \lambda \kappa v_k^2 d_k d_k^\dagger + \lambda^2 \kappa^2 v_k^4 d_{N-k} d_{N-k}^\dagger d_k d_k^\dagger - \lambda^2 \kappa^2 v_k^2 u_k^2 d_{N-k} d_k d_{N-k}^\dagger d_k^\dagger.$$

Elementary calculations using the relations (24) and (25) yield

$$\mathcal{Q}(\lambda) = \prod_{k=1}^{N/2} (1 - 2\lambda \kappa v_k^2 + \lambda^2 \kappa^2 v_k^2). \quad (26)$$

At this point it is convenient to introduce the distribution function $p(m, M)$ of counting m particles for $M/2$ pairs of modes. This is the topic of the next section.

C. Counting statistics

The counting distribution is calculated from the generating function by the relation in Eq. (18). We use the generalized Leibniz rule

$$\frac{d^m}{d\lambda^m} \prod_{k=1}^N f_k(\lambda) = \sum_{n_1 + \dots + n_N = m} \binom{m}{n_1, n_2, \dots, n_N} \prod_{k=1}^N \frac{d^{n_k}}{d\lambda^{n_k}} f_k(\lambda),$$

where the generalized Newton symbol is given by

$$\binom{m}{n_1, n_2, \dots, n_N} = \frac{m!}{n_1! n_2! \dots n_N!},$$

to derive a recurrence relation, to calculate the distribution for $(M+1)$ modes, given the distribution for M modes.

The distribution function $p(m, M)$ for M modes is given by

$$\begin{aligned} p(m, M) &= \frac{(-1)^m}{m!} \frac{d^m}{d\lambda^m} \mathcal{Q} \Big|_{\lambda=1} \\ &= \frac{(-1)^m}{m!} \sum_{l_1, l_2, \dots, l_N} \frac{m!}{l_1! l_2! \dots l_N!} \prod_{j=1}^{M/2} \frac{d^{l_j}}{d\lambda^{l_j}} (1 - 2\lambda \kappa v_k^2 + \lambda^2 \kappa^2 v_k^2), \end{aligned} \quad (27)$$

where the summation runs over l_1, \dots, l_M such that $l_1 + \dots + l_M = m$, where $l_j = 0, 1, \text{ or } 2$, for $j = 1, \dots, M$.

We can now derive the recursive relation

$$p(m, M+1) = \sum_{i=0}^2 \mathcal{P}_i p(m-i, M), \quad (28)$$

where

$$\begin{aligned} \mathcal{P}_0 &= 1 - 2\kappa v_{M+1}^2 + \kappa^2 v_{M+1}^2, \\ \mathcal{P}_1 &= 2\kappa v_{M+1}^2 - 2\kappa^2 v_{M+1}^2, \\ \mathcal{P}_2 &= 1 - \mathcal{P}_0 - \mathcal{P}_1 \end{aligned} \quad (29)$$

are the probabilities of detecting 0, 1, or 2 particles in the modes $M+1$ and $N-M-1$. Therefore, starting from $p(0, 1) = 1 - 2\kappa v_1^2 + \kappa^2 v_1^2$, $p(1, 1) = 2\kappa v_1^2$, and $p(2, 1) = \kappa v_1^2$, we can use the recurrence relation (28) to calculate the counting distribution for an arbitrary number of modes.

Let us turn now to our results and discuss the counting statistics for different values of γ . In the figures that we plot

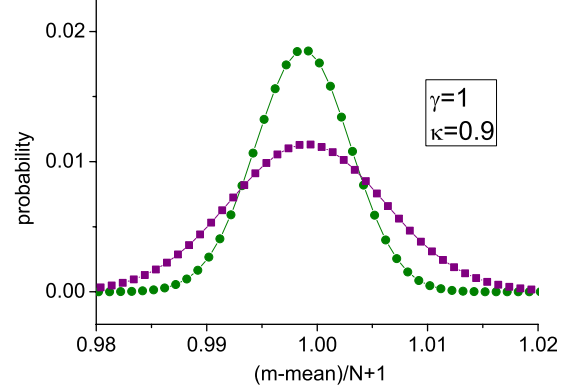


FIG. 1. (Color online) Counting statistics of the transverse Ising model ($\gamma=1$). The horizontal axis is of $(m-\bar{m})/N+1$, and has units of particles per lattice site. The means \bar{m} of the corresponding distributions are denoted by “mean” in the figure. The vertical axis is of the corresponding probability. The curve with purple squares is for $h/J=0.01$, while the one with green circles is for $h/J=10$. The quantum phase transition (QPT) of this model is at $h/J=1$. Both the distributions are sub-Poissonian. However, the counting distribution becomes much narrower in the case when $h/J > 1$ than when $h/J < 1$. In this case, we have taken the efficiency κ as 0.9.

below (except in Fig. 6 in Sec. III G), we choose a value of the total number of modes, N , such that the corresponding quantities (distribution, mean, variance, etc.) have already converged. In the cases that we consider, such convergence occurs for $N \approx 300$.

D. Transverse Ising model

The counting distributions for the transverse Ising model (transverse XY model with $\gamma=1$) for two exemplary values of the field parameter $g=h/J$ are shown in Fig. 1. The Ising model has a quantum phase transition at $g=1$ [12], and one exemplary value of g is chosen below the QPT, and the other above it. The difference in behavior is clearly seen. (\bar{m} and σ^2 denote the mean and variance of the distribution, respectively.) Below, it will be more clearly revealed by looking at the mean and the variance of the distribution.

E. Transverse XY model: Transition anisotropy

In Fig. 2, we plot counting distributions as a function of

$$\frac{m-\bar{m}}{N} + 1, \quad (30)$$

for four values of γ , for a fixed value of the efficiency $\kappa = 0.9$, and for two extreme values of g : $g \rightarrow 0$ and $g \rightarrow \infty$. Note that all the distributions presented in Fig. 2 are smooth and their widths ($\approx \sqrt{\sigma^2}/N$) are of order of 0.01. Since, as we argue below, $\bar{m} \approx \kappa N$, all the distributions are sub-Poissonian, because $\sigma^2 \leq \bar{m}$, despite the finite detection efficiency. For $\gamma \rightarrow 0$, the distribution for $g \rightarrow 0$ is narrower than that for $g \rightarrow \infty$. This tendency is inverted in the Ising model, when the distribution for $g \rightarrow 0$ has a larger variance than the one for $g \rightarrow \infty$. At what we call the *transition anisotropy* γ

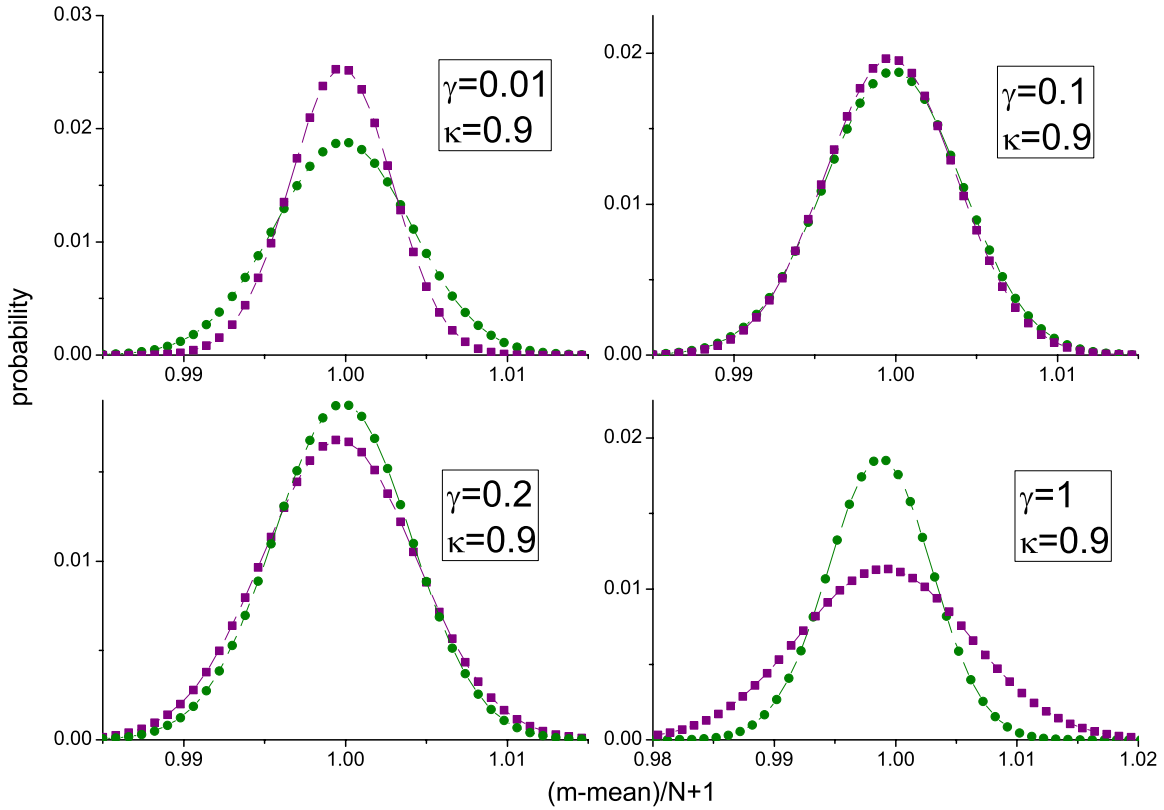


FIG. 2. (Color online) Fermion-counting distribution as a function of $(m-\bar{m})/N+1$ (horizontal axis, with units of particles per lattice site) for $\kappa=0.9$, and for the indicated values of γ . Purple squares correspond to $h/J \rightarrow 0$, and green circles to $h/J \rightarrow \infty$. The transition anisotropy is here at $\gamma \approx 0.1$. The means \bar{m} of the corresponding distributions are denoted by “mean” in the figure.

≈ 0.1 , the distributions for $g \rightarrow 0$ and $g \rightarrow \infty$ practically coincide.

This transition anisotropy depends on the efficiency κ , and it moves to $\gamma \rightarrow 0$, as $\kappa \rightarrow 1$. This indicates that the probability distribution of counting can distinguish the two universality classes (the XX, with $\gamma=0$, and the Ising, with $\gamma > 0$) among the XY models on a chain. In the limit of $\kappa \rightarrow 1^-$, only the model with $\gamma \rightarrow 0$ has lower variance for $g \rightarrow 0$ as compared to $g \rightarrow \infty$, while all the other XY models (with $\gamma \neq 0$) have the opposite behavior.

F. Recurrence relations for mean and variance

In order to understand the properties of counting distributions better, we look at the mean and variance, which can be calculated from the following recurrences, which are obtained from the recurrence relation given in Eq. (28):

$$\overline{m_{M+1}} = \overline{m_M} + 2\kappa v_{M+1}^2, \tag{31}$$

$$\sigma_{M+1}^2 = \overline{m_{M+1}^2} - \overline{m_{M+1}}^2 = \sigma_M^2 + 4\kappa^2 v_{M+1}^2 (1 - v_{M+1}^2). \tag{32}$$

To obtain the relation (31), one multiplies both sides of the recurrence (28) by m , and sums over m , and some further simple algebraic manipulations. Relation (32) is obtained similarly by a multiplication of m^2 on both sides of Eq. (28). Since $\overline{m_1}$ and σ_1^2 can be trivially calculated, the mean and variance can be obtained by these relations for an arbitrary number of modes. The recurrences imply that the mean m_N

$\leq \kappa N$; we find the typical value of $\overline{m_N}$ indeed to be of order of κN . On the other hand, the variance $\sigma_N^2 \leq \kappa^2 N$. Both quantities show singular behavior in the thermodynamical limit at criticality. In particular, for the transverse Ising model ($\gamma = 1$), near the critical point $g = g_c \equiv 1$, the mean \bar{m} can be written in terms of elliptic integrals of first and second kind, and can be expressed as [32] (see [12,27] and references therein)

$$\bar{m} \approx -\frac{1}{2\pi}(g - g_c) \ln|g - g_c| - \frac{1}{\pi},$$

so that

$$d\bar{m}/dg \approx -(\ln|g - g_c| + 1)/2\pi.$$

Since all models with $\gamma \neq 0$ belong to the same universality class, they all present the same singular behavior [12]. This is contrasted with the case of XX model, which belongs to a different universality class. The singular behavior is clearly seen in the plots of \bar{m}/N and σ^2/N obtained for finite $N \approx 300$ and ideal $\kappa=1$ (see Fig. 3). For finite values of γ , the variance shows a jump in the first derivative, while the first derivative of the mean tends to “infinity” at g_c . This behavior is better seen when one plots directly the derivatives of \bar{m} and σ^2 (see Fig. 4). This behavior changes drastically as $\gamma \rightarrow 0$. The variance tends then to zero (in the symmetric XX model the particle number is conserved), and the mean has a diverging derivative for $g < g_c$, and is constant for $g > g_c$.

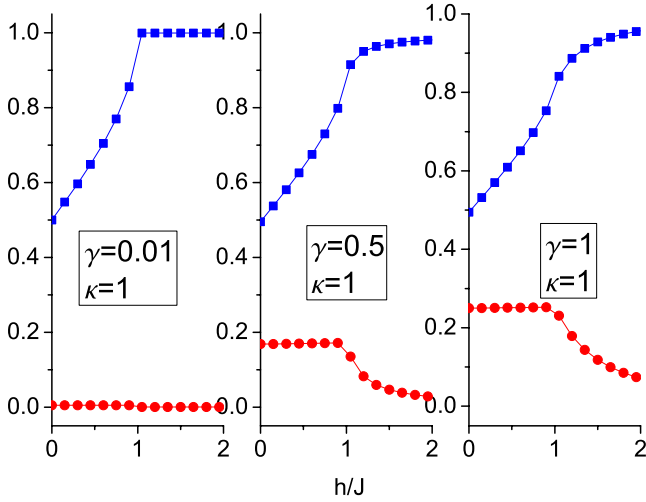


FIG. 3. (Color online) Mean \bar{m}/N (blue squares) and variance σ^2/N (red circles) of the fermion-counting distribution as a function of $g=h/J$ for $\kappa=1$, and indicated values of γ . Horizontal axes: the dimensionless quantity g . Vertical axes: mean for the blue squares, and variance for the red circles (always with units of particles per lattice site).

Amazingly, although finite detector efficiency obviously smooths out the curves, the signatures of the singularities are clearly visible even for $\kappa=0.5$ (see Fig. 5). A clear change of behavior of the curves is visible even at $\kappa=0.1$. Note that in all considered cases so far, the variance $\sigma^2/N < \bar{m}/N$, i.e., all distributions are sub-Poissonian. Note, however, that going from the antiferromagnetic to the ferromagnetic case does not affect the variance, but replaces $\bar{m}/N \rightarrow (1/2 - \bar{m}/N)$. In that case, we do observe a transition from sub-Poissonian behavior at small g , to (weakly) super-Poissonian for large g . Let the value of g at the transition be g_t ; g_t tends to g_c from below, as $\gamma \rightarrow 0$.

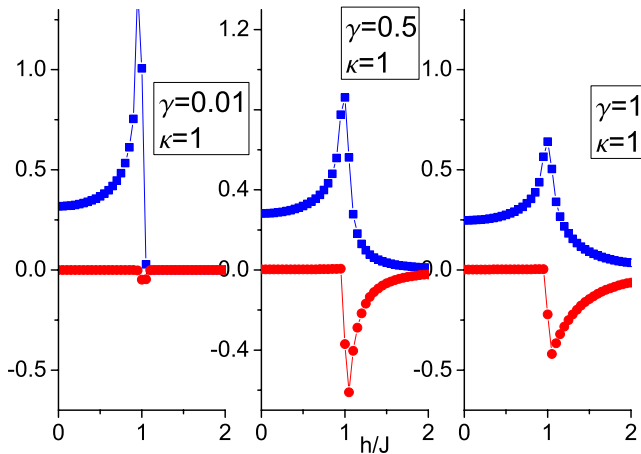


FIG. 4. (Color online) Derivatives of the means and variances vs the transverse field $g=h/J$, for $\gamma=0.01$, 0.5, and 1. Blue squares denote the derivatives of the means, while red circles denote the derivatives of the variances, in the respective cases. Also, $\kappa=1$. The QPTs of all the models at $g=1$ are clearly visible. Horizontal axes: the dimensionless quantity g . Vertical axes: the derivatives of the mean for the blue squares, and of the variance for the red circles (always with units of particles per lattice site).

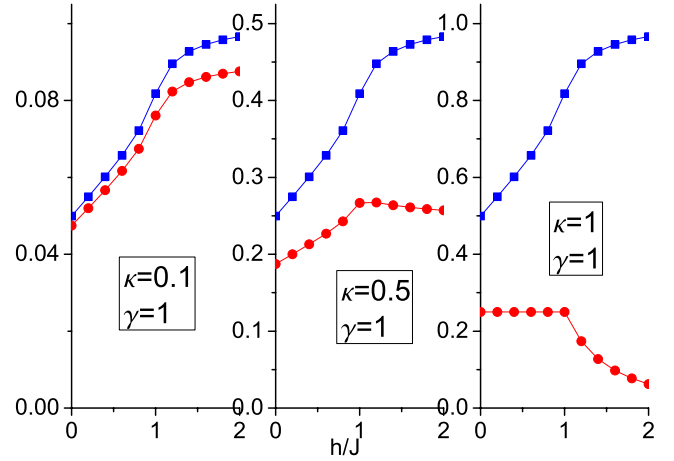


FIG. 5. (Color online) Mean \bar{m}/N (blue squares) and variance σ^2/N (red circles) of the fermion-counting distribution as a function of $g=h/J$ for $\gamma=1$ (Ising model), and indicated values of κ . Horizontal axes: are the dimensionless quantity g . Vertical axes: the mean for the blue squares, and the variance for the red circles (always with units of particles per lattice site).

G. Even versus odd splitting

The Bogoliubov transformation used to solve the models considered can be regarded as a “squeezing” or “pairing” transformation. The ground state that we investigated is analogous to the BCS state of semiconductors, i.e., they involve fermion (Cooper-like) pairs. Thus, in the ideal case of $\kappa=1$, the counting distributions are exactly zero for odd numbers of particles. In practice, for finite values of N and $\kappa < 1$, the distributions oscillate between larger values for even, and small for odd number of counts. This behavior is very strongly affected by $\kappa < 1$, since at finite efficiency, one may easily miss single atoms from the Cooper pairs, and obtain odd counts. In effect, for a given value of N , the even-odd asymmetry is visible only for κ close enough to 1. Similarly, the even-odd asymmetry is strongly affected by the finite size effects—for a given value of $\kappa < 1$ it is visible only for N small enough (see Fig. 6). Similar behavior has also been observed in Ref. [13].

H. Counting spatial Fourier components of the fermion density

Finally, let us point out that the methods proposed in [11] allow for measurements of various kinds of Fourier components of the total spin. In terms of particle counting, these methods allow, for instance, the counting of particles in every second site, every third site, etc. Our theory is easily generalized to such situations.

In the case when we count every second c fermion, we have to express $b_{2j}^\dagger b_{2j} = c_{2j}^\dagger c_{2j}$ in terms of the d fermions. As before, as a first step we do the Fourier transform

$$c_{2j}^\dagger = \sum_{k=0}^{N-1} \exp(-2ij\Phi_k) a_k^\dagger,$$

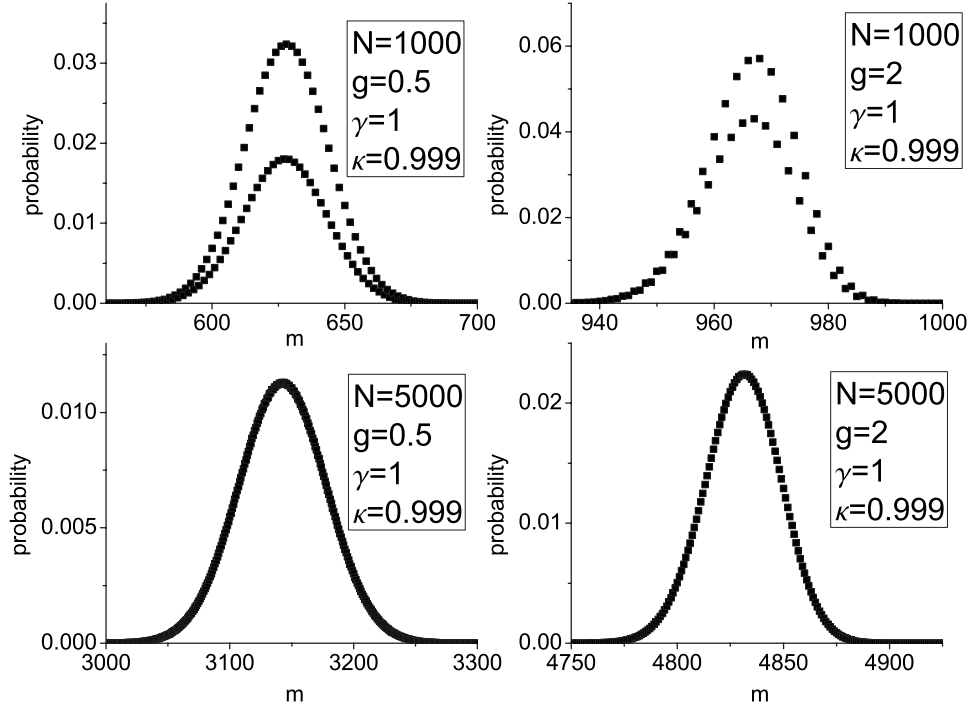


FIG. 6. Even versus odd splitting for $\kappa=0.999$ in the Ising model. For $N=1000$ the probability distribution splits up, whereas for $N=5000$ there is virtually no splitting. Note that $g=h/J$. Horizontal axes: the quantity m in units of particles. Note that the lower curves are those for odd m .

$$c_{2j} = \sum_{k=0}^{N-1} \exp(+2ij\Phi_k) a_k. \quad (33)$$

The expression $\sum_{j=0}^{N/2-1} c_{2j}^\dagger c_{2j} = \frac{1}{2} \sum_{j=0}^{N-1} c_{2j}^\dagger c_{2j}$ can thus be written as

$$\sum_{j=0}^{N/2-1} c_{2j}^\dagger c_{2j} = \frac{1}{2} \sum_{k,k'} \frac{1 - \exp[4\pi i(k-k')]}{1 - \exp[4\pi i(k-k')/N]} a_k^\dagger a_{k'}, \quad (34)$$

which is nonvanishing for $k-k'=0$ or $|k-k'|=N/2$. Finally,

$$\begin{aligned} \sum_{j=0}^{N/2-1} c_{2j}^\dagger c_{2j} &= \frac{1}{2} \sum_{j=0}^{N/2-1} a_k^\dagger a_k + a_{k+N/2}^\dagger a_{k+N/2} + a_k^\dagger a_{k+N/2} + a_{k+N/2}^\dagger a_k \\ &= \frac{1}{2} \sum_{j=0}^{N/2-1} (a_k^\dagger + a_{k+N/2}^\dagger)(a_k + a_{k+N/2}). \end{aligned} \quad (35)$$

We can now calculate $\mathcal{Q}(\lambda)$ as follows:

$$\begin{aligned} \mathcal{Q}(\lambda) &= \text{Tr} \left(\rho: \prod_{k=0}^{N/2-1} e^{-1/2\lambda\kappa(a_k^\dagger + a_{N/2+k}^\dagger)(a_k + a_{N/2+k})} : \right) \\ &= \prod_{k=0}^{N/2-1} \left(1 - \frac{1}{2} \lambda \kappa (a_k^\dagger + a_{N/2+k}^\dagger)(a_k + a_{N/2+k}) \right) \\ &= \prod_{k=1}^{N/4} \left[\left(1 - \frac{1}{2} \lambda \kappa (a_k^\dagger + a_{N/2+k}^\dagger)(a_k + a_{N/2+k}) \right) \right. \end{aligned}$$

$$\left. \times \left(1 - \frac{1}{2} \lambda \kappa (a_{N-k}^\dagger + a_{N/2-k}^\dagger)(a_{N-k} + a_{N/2-k}) \right) \right]. \quad (36)$$

After performing the Bogoliubov transform, and keeping the relevant terms for the vacuum state of the d fermions, the generating function \mathcal{Q} is given by

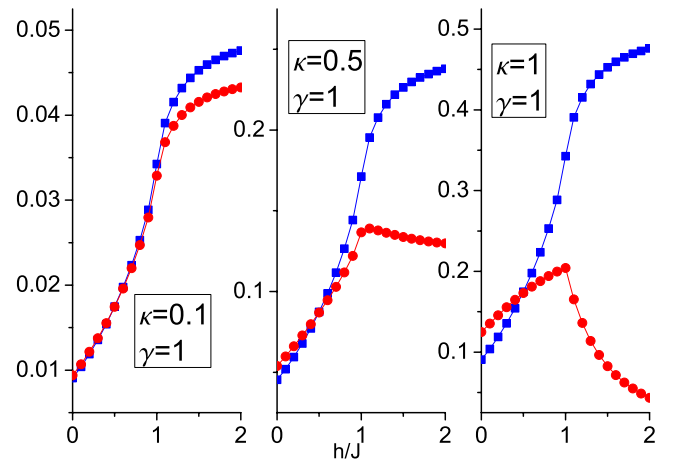


FIG. 7. (Color online) Mean \bar{m}/N (blue squares) and variance σ^2/N (red circles) of the counting distribution of every second fermion as a function of $g=h/J$ for $\gamma=1$ (Ising model), and indicated values of κ . Horizontal axes: the dimensionless quantity g . Vertical axes: the mean for the blue squares, and the variance for the red circles (always with units of particles per lattice site).

$$\mathcal{Q}(\lambda) = \prod_{k=1}^{N/4} (1 - 2\lambda\kappa v_k^2 + \lambda^2\kappa^2 v_k^2), \quad (37)$$

which is in the same form as in Eq. (26), with the product restricted, however, to $N/4$ terms. We then easily derive analogous recurrences as in the cases considered so far. Figure 7 shows the behavior of the mean and the variance, when every second spin is counted, in the transverse Ising model. Note that the traces of singular behavior at $g=g_c$ persist. What is perhaps more interesting is that the general behavior is more rich. In particular, there is a crossing from sub-to super-Poissonian behavior at $g=0.5$. For $\gamma \rightarrow 0$ the point of crossing moves to zero, and the variance disappears.

IV. SUMMARY

Summarizing, we have formulated and applied fermion- and spin-counting theory to a family of one-dimensional

strongly correlated systems that can be realized and detected with ultracold atoms. The counting distributions exhibit traces of singularities at criticality, that persist even at low detection efficiencies. They show various kinds of rich behavior, such as transitions from sub-to super-Poissonian character, and even-odd oscillations.

ACKNOWLEDGMENTS

We acknowledge support from the Spanish MEC (Grant No. FIS-2005-04627, Consolider Ingenio QOIT, Acciones Integradas, and Ramón y Cajal), Caixa Manresa, DAAD (German Academic Exchange Service), ESF (Program QUDEDIS), MEC/ESF (Program Euroquam FERMIX), the Ministry of Education of the Generalitat de Catalunya, and EU IP SCALA.

-
- [1] R. J. Glauber, in *Quantum Optics and Electronics*, edited by B. DeWitt, C. Blandin, and C. Cohen-Tannoudji (Gordon and Breach, New York, 1965), pp. 63–185.
- [2] M. Yasuda and F. Shimizu, *Phys. Rev. Lett.* **77**, 3090 (1996).
- [3] M. Schellekens, R. Hoppeler, A. Perrin, J. Viana Gomes, D. Boiron, A. Aspect, and C. I. Westbrook, *Science* **310**, 648 (2005).
- [4] T. Jelts, J. M. McNamara, W. Hogervorst, W. Vassen, V. Krachmalnicoff, M. Schellekens, A. Perrin, H. Chang, D. Boiron, A. Aspect, and C. I. Westbrook, *Nature (London)* **445**, 402 (2007).
- [5] A. Öttl, S. Ritter, M. Köhl, and T. Esslinger, *Phys. Rev. Lett.* **95**, 090404 (2005).
- [6] M. Lewenstein, *Nature (London)* **445**, 372 (2007).
- [7] A. Imambekov, V. Gritsev, and E. Demler, in *Ultracold Fermi Gases*, Proceedings of the International School of Physics “Enrico Fermi,” 2006 (IOS Press, 2006); A. Polkovnikov, *Europhys. Lett.* **78**, 10006 (2007).
- [8] J. L. Sørensen, J. Hald, and E. S. Polzik, *Phys. Rev. Lett.* **80**, 3487 (1998).
- [9] K. Eckert, Ł. Zawitkowski, A. Sanpera, M. Lewenstein, and E. S. Polzik, *Phys. Rev. Lett.* **98**, 100404 (2007).
- [10] M. Born and E. Wolf, *Principles of Optics: Electromagnetic Theory of Propagation, Interference and Diffraction of Light* (Cambridge University Press, Cambridge, U.K., 1999).
- [11] K. Eckert, O. Romero-Isart, M. Rodríguez, M. Lewenstein, E. S. Polzik, and A. Sanpera, *Nat. Phys.* **4**, 50 (2008).
- [12] S. Sachdev, *Quantum Phase Transitions* (Cambridge University Press, Cambridge, U.K., 2001).
- [13] R. W. Cherg and E. Demler, *New J. Phys.* **9**, 7 (2007).
- [14] K. E. Cahill and R. J. Glauber, *Phys. Rev. A* **59**, 1538 (1999).
- [15] F. Hassler, M. V. Suslov, G. M. Graf, M. V. Lebedev, G. B. Lesovik, and G. Blatter, *Phys. Rev. B* **78**, 165330 (2008).
- [16] L. S. Levitov, H. Lee, and G. B. Lesovik, *J. Math. Phys.* **37**, 4845 (1996); G. B. Lesovik, F. Hassler, and G. Blatter, *Phys. Rev. Lett.* **96**, 106801 (2006).
- [17] W. Belzig, C. Schroll, and C. Bruder, *Phys. Rev. A* **75**, 063611 (2007).
- [18] S. Staudenmayer, W. Belzig, and C. Bruder, *Phys. Rev. A* **77**, 013612 (2008).
- [19] M. Lewenstein, L. Santos, M. A. Baranov, and H. Fehrmann, *Phys. Rev. Lett.* **92**, 050401 (2004).
- [20] A. J. Leggett, *Quantum Liquids* (Oxford University Press, New York, 2006).
- [21] M. Lewenstein, A. Sanpera, V. Ahufinger, B. Damski, A. Sen(De), and U. Sen, *Adv. Phys.* **56**, 243 (2007).
- [22] U. Dörner, P. Fedichev, D. Jaksch, M. Lewenstein, and P. Zoller, *Phys. Rev. Lett.* **91**, 073601 (2003).
- [23] A. Auerbach, *Interacting Electrons and Quantum Magnetism* (Springer, New York, 1994).
- [24] M. Anderlini, P. J. Lee, B. L. Brown, J. Sebby-Strabley, W. D. Phillips, and J. V. Porto, *Nature (London)* **448**, 452 (2007).
- [25] S. Trotzky, P. Cheinet, S. Fölling, M. Feld, U. Schnorrberger, A. M. Rey, A. Polkovnikov, E. A. Demler, M. D. Lukin, and I. Bloch, *Science* **319**, 295 (2008).
- [26] J. Wehr, A. Niederberger, L. Sanchez-Palencia, and M. Lewenstein, *Phys. Rev. B* **74**, 224448 (2006).
- [27] S. Katsura, *Phys. Rev.* **127**, 1508 (1962); P. Pfeuty, *Ann. Phys. (N.Y.)* **57**, 79 (1970); E. Lieb, T. Schultz, and D. Mattis, *ibid.* **16**, 407 (1961); E. Barouch, B. M. McCoy, and M. Dresden, *Phys. Rev. A* **2**, 1075 (1970); E. Barouch and B. M. McCoy, *ibid.* **3**, 786 (1971); **3**, 2137 (1971).
- [28] J. Grochmalicki and M. Lewenstein, *Phys. Rep.* **208**, 189 (1991).
- [29] M. Le Berre, in *Photons and Quantum Fluctuations*, edited by E. R. Pike and H. Walther (Hilger, Bristol, 1988).
- [30] W. Vogel, D.-G. Welsch, and S. Wallentowitz, *Lectures in Quantum Optics: An Introduction* (Wiley, Berlin, 2001).
- [31] J. Sherson, B. Julsgaard, and E. S. Polzik, *Adv. At., Mol., Opt. Phys.* **54**, 81 (2006); K. Hammerer, K. Mølmer, E. S. Polzik, and J. I. Cirac, *Phys. Rev. A* **70**, 044304 (2004); K. Eckert, O. Romero-Isart, M. Rodríguez, M. Lewenstein, E. S. Polzik, and A. Sanpera, *Nat. Phys.* **4**, 50 (2008).
- [32] I. S. Gradshteyn and I. M. Ryzhik, *Table of Integrals, Series, and Products* (Academic Press, San Diego, 2000).